Surface plasmon polariton analogue to Young's double-slit experiment

RASHID ZIA† AND MARK L. BRONGERSMA*

Geballe Laboratory for Advanced Materials, Stanford University, Stanford, California 94305, USA
†Present address: Division of Engineering, Brown University, Providence, Rhode Island 02912, USA
*e-mail: brongersma@stanford.edu

Published online: 1 July 2007; doi:10.1038/nnano.2007.185

When a light wave strikes a metal film it can, under appropriate conditions, excite a surface plasmon polariton (SPP)—a surface electromagnetic wave that is coupled to the free electrons in the metal. Such SPPs are involved in a wide range of phenomena[1], including nanoscale optical waveguiding[2–5], perfect lensing[6], extraordinary optical transmission[7], subwavelength lithography[8] and ultrahigh-sensitivity biosensing[9]. However, before the full potential of technology based on SPPs (termed 'plasmonics') can be realized, many fundamental questions regarding the interaction between light and matter at the nanoscale need to be answered. For over 200 years, Young's double-slit experiment has been a valuable pedagogical tool for demonstrating the wave nature of light[10]. Here, we perform a double-slit experiment with SPPs to reveal the strong analogy between SPP propagation along the surface of metallic structures and light propagation in conventional dielectric components (such as glass waveguides). This allows us to construct a general framework to describe the propagation, diffraction and interference of SPPs. It also suggests that there is an effective diffraction limit for the lateral confinement of SPPs on metal stripe waveguides, and justifies the use of well-developed concepts from conventional optics and photonics in the design of new plasmonic devices.

Figure 1a shows a schematic of the experimental configuration used to visualize and study the interplay between SPP propagation, diffraction and interference. Using electron-beam lithography, a 48-nm-thick Au film was patterned on a glass substrate to form two metal stripe waveguides protruding from an extended metal film region called the launchpad. The two stripes play a role analogous to the two slits in the traditional double-slit experiment using light. The stripes are 2 μm wide, separated by a gap of 2 μm, and they terminate in another extended thin-film region called the termination pad. Similar to previous experimental studies[11–13], a photon scanning tunnelling microscope (PSTM) is used to visualize the SPP propagation; the details of our particular system are described in detail elsewhere[13]. In short, an apertured cantilever probe, shown schematically in Fig. 1a, is used locally to tap into the guided SPP waves and scatter light towards a photodetector in the far field. The probes used in this study have a nanoscale aperture, defined at the end of a pyramidal tip, through which light can be collected. The detected signal provides a measure of the local field intensity directly under the tip, and the propagation of the SPPs is imaged by scanning the tip over the metal structure. In contrast to earlier double-slit experiments with light, electrons[14] and atoms[15], a PSTM has the unique ability to directly image the diffraction and interference of these surface electromagnetic waves at the nanoscale and at arbitrary distances from the slits, whereas in many experiments the interference can only be observed using a screen at a fixed distance from the slits. It should be noted that in the classic Young's double-slit experiment with light, SPPs also play an essential role[16]. The current study distinguishes itself from earlier studies by focusing on pure SPP diffraction.

Several numerical techniques were used to simulate guiding along the two metal stripes and the subsequent diffraction and interference in the extended metal film regions. In previous numerical and experimental studies[13,17], we have shown that the 2-μm-wide stripe waveguides used in this study only support a single quasi-transverse magnetic (TM) leaky SPP mode. It is important to realize that this experiment could not have been performed on substantially narrower stripes, as such stripes exhibit cutoff[13]; that is, they do not support leaky TM SPP modes. The experiments could have been performed on wider stripes, but the observed diffraction would have been weaker and the analysis would have been more complicated because of the presence of higher-order leaky TM modes. Figure 2a shows the mode profile appropriate for the 2-μm stripe as calculated by the full-vectorial finite-difference method described in ref. 17. This mode appears localized at the top air–metal interface, but leakage radiation extends into the high-index glass substrate, hence the term 'leaky mode'. Similar behaviour is observed for the leaky SPPs supported by the infinitely wide 48-nm thin film shown in Fig. 2b (ref. 18). Although these modes can be calculated numerically, their leaky nature precludes a straightforward normalization procedure in the vertical dimension. For this reason, the coupling between stripe and film modes cannot be determined rigorously by conventional overlap integral methods. We suggest a method to circumvent this problem and show how the diffraction and interference of SPPs can be simulated using a simple scalar diffraction model.

To simulate the double-slit diffraction experiment, we make use of recent work validating a dielectric waveguide model for guided SPPs on a metal stripe[19]. First, this model is used to solve for the SPP mode supported by the metal stripe waveguides. The calculated lateral mode profile is then used as the input for a proposed scalar diffraction model, which will be shown to accurately predict the diffraction pattern imaged by PSTM. The successful prediction of the diffraction pattern based on the guiding properties of the stripes provides evidence for the

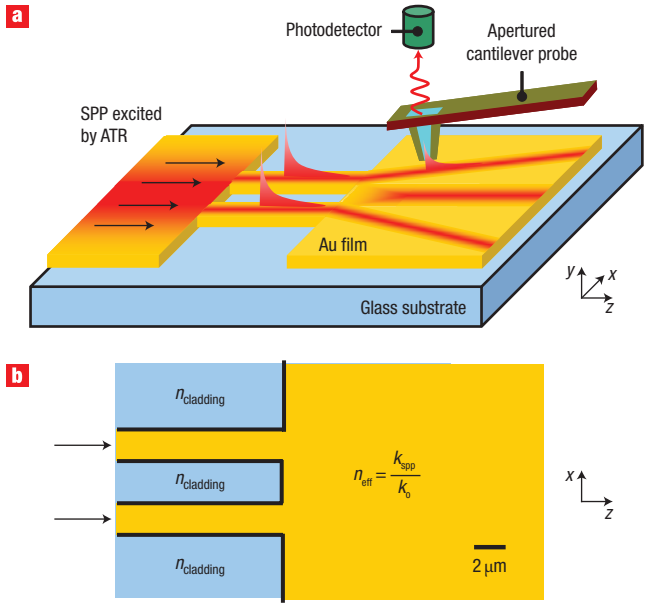

Figure 1 Schematic of a double-slit experiment for surface plasmon polaritons (SPPs). a, Schematic of an experimental configuration in which a PSTM is used to visualize Young's double-slit experiment for SPPs. The SPPs are first launched along the surface of a patterned Au film (on the left) by an attenuated total reflection technique. These SPPs then excite the guided polariton modes supported by two adjacent metal stripe waveguides. These stripes perform an analogous role to the slits in the traditional Young's double-slit experiment. An apertured cantilever probe is used to locally tap into the guided SPP waves and scatter light towards a photodetector in the far field. The detected signal provides a measure of the local field intensity just under the tip and the propagation, diffraction and interference of the SPPs can be imaged by scanning the tip over the patterned metal. **b**, Schematic of the equivalent dielectric structure used to model SPP propagation and diffraction.

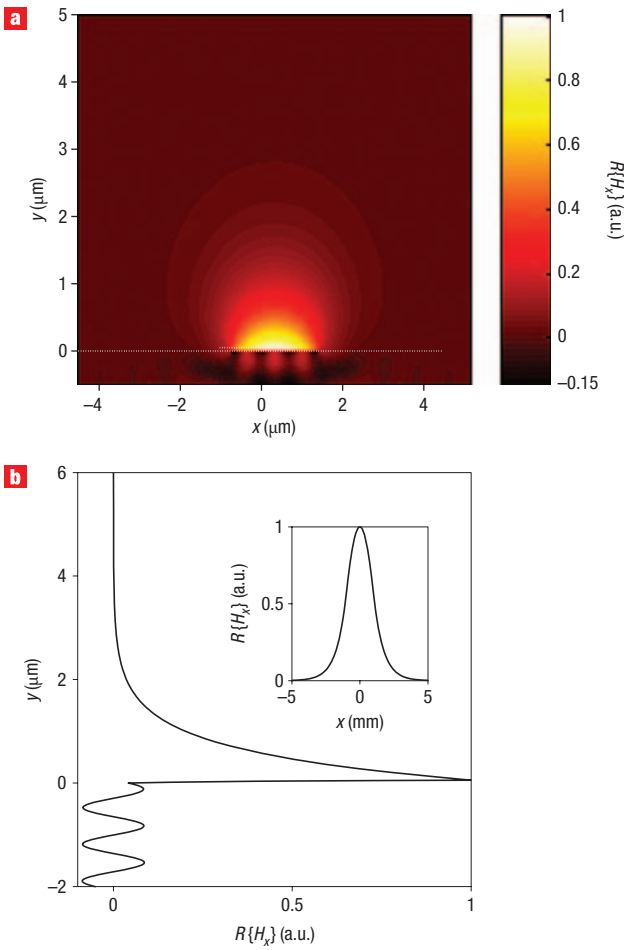

Figure 2 Electromagnetic simulation of the leaky surface plasmon polariton (SPP) mode supported by the two metal stripes used in the double-slit experiment. a, Exact numerical solution for the leaky SPP mode supported by a 2-μm-wide (*x*-direction) and 48-nm-thick (*y*-direction) Au stripe on a glass substrate. The simulation shows the real part of the dominant *x*-component of the magnetic field, $R\{H_x\}$, as a function of *x* and *y*. **b**, Approximate solutions for the leaky SPP mode supported by the same metal stripes as discussed in **a**. The mode profiles were calculated using the dielectric waveguide model presented in the main text. The simulation shows $R\{H_x\}$ as a function of *y* and the inset shows the dependence of $R\{H_x\}$ on *x*.

existence of a general framework that treats SPP guiding, diffraction and interference on the same basis.

The dielectric waveguide model in ref. 19 is an effective index method for surface plasmon waveguides[2,20,21] because it approximates the complex three-dimensional eigenvalue problem by solving for the modes of two independent slab waveguides. Along the vertical (*y*) direction, one can make use of the fact that the guided mode closely resembles the SPP supported by an infinitely wide metal film and solve for the vertical mode profile and propagation constant, k_{spp}, of an air–Au–glass metallic slab waveguide (see Fig. 2b). For the lateral direction, it was shown that the mode profile resembles the fundamental transverse electric (TE) mode of an equivalent dielectric slab waveguide as shown in the inset of Fig. 2b (ref. 19). The core index for the slab is determined by the effective index appropriate to an SPP on an infinitely wide film ($n_{eff} = k_{spp}/k_0 = 1.02215 + i * 0.003066$; ref. 22), and the cladding index is determined by the surrounding material (air).

By independently solving for the lateral and vertical mode profiles, this model isolates the leaky nature of the guided modes to the vertical dimension, and thus produces a lateral profile that may be normalized. In the lateral direction, the optical modes are decomposed into the SPPs supported by an infinitely wide film with a well-defined in-plane momentum (k_{spp}, where $k_x^2 + k_z^2 = k_{spp}^2$). In analogy to dielectric photonics, this momentum, k_{spp}, is assumed to be a conserved quantity throughout the entire guiding and subsequent diffraction process. This notion of momentum conservation allows for a straightforward simulation of the diffraction pattern using scalar diffraction theory[23]. In doing so, the lateral field profile, $\psi(x)$, predicted by the equivalent dielectric waveguide model, is first expanded into an angular spectrum of SPPs, $A(k_x)$:

$$A(k_x) = \int_{-\infty}^{\infty} \psi(x) e^{-ik_x x}\, dx$$

This equation describes the amplitude and phase of SPPs at the interface between the waveguides and the extended film. Next, this angular spectrum is propagated forward in a manner

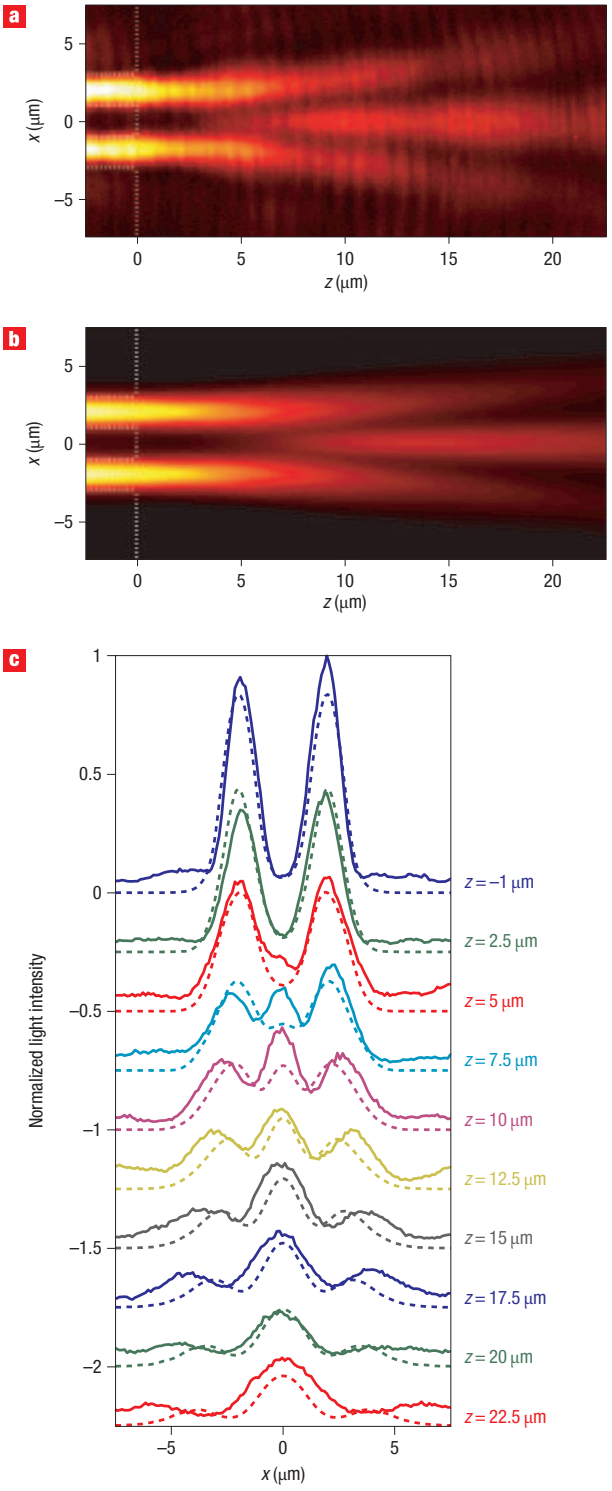

Figure 3 Double-slit experiment and simulation. a, Experimental near-field image taken with a PSTM demonstrating guided polariton propagation, diffraction and interference for the structure shown in Fig. 1a. **b**, Light intensity image predicted by numerical simulations of the equivalent dielectric structure shown in Fig. 1b. **c**, Comparison of lateral cross-sections for experimental data (solid lines) and results of simulations (dashed lines) with plots offset by −0.25 increments along the *y*-axis. The dashed white lines in panels **a** and **b** mark the edges of the metal film and model structure, respectively. The experimental data show an offset due to background noise that has not been subtracted.

analogous to the propagation of plane waves in a uniform dielectric region of refractive index as follows:

$$\psi(x,z) = \frac{1}{2\pi}\int_{-\infty}^{\infty} A(k_x)\mathrm{e}^{ik_x x}\mathrm{e}^{iz\sqrt{k_{spp}^2-k_x^2}}\,\mathrm{d}k_x$$

Note that the critical assumption of momentum conservation is equivalent to assuming a constant effective index $n_{eff} = k_{spp}/k_0$ for the entire metal structure. Hence, by analogy, this scalar method models the experimental configuration shown in Fig. 1a with the equivalent dielectric structure shown in Fig. 1b.

The near-field intensity recorded by our PSTM is presented in Fig. 3a. The light intensity distribution closely resembles the well-known diffraction and interference pattern of Young's original double-slit experiment. Following a region of lateral confinement along the metal stripes ($z < 0$), SPPs diffract into the extended termination pad region ($z > 0$), and where the diffracted beams overlap, an interference pattern is observed. This interference pattern is characterized by a central maximum due to the constructive interference of the SPPs emitted by adjacent waveguides. The experimental image is in good agreement with the prediction of our equivalent dielectric model (Fig. 3b). This is further illustrated in Fig. 3c, which shows lateral cross-sections taken from the experimental and simulated images in Fig. 3a,b, respectively. They clearly illustrate how the double-peaked intensity distribution changes into a three-peaked distribution. A comparison between the experimental (solid lines) and simulated (dashed lines) lateral cross-sections in Fig. 3c shows that our model accurately predicts the observed lateral mode profile above the metal stripes as well as the subsequent diffraction and interference peaks above the extended metal pad.

The agreement between experiment and theory suggests that our basis set for scalar diffraction is appropriate and that the guided modes of a finite-width metal stripe can be decomposed into an angular spectrum of SPPs supported by an extended metal film. Moreover, our results also suggest that there is an effective diffraction limit for metal stripe waveguides by which the lateral mode size is limited to $\Delta x \geq \lambda_0/2n_{eff}$ (ref. 19). Given the complex boundary conditions that exist at the edge of a metal stripe, the existence of such a diffraction limit has been a topic of considerable contention (see Supplementary Information). In the context of electromagnetic theory, however, it is not surprising that SPPs can be well modelled by scalar wave theory. Indeed, the boundary conditions that support SPPs at a metal–dielectric interface specifically allow for only TM waves. Therefore, any surface plasmon mode on a finite-width interface must represent a superposition of TM surface waves just as the guided mode of a dielectric waveguide represents a superposition of transverse electromagnetic (TEM) volume waves.

In conclusion, we have constructed and experimentally verified a general framework for the guiding, diffraction and interference of SPPs on patterned metal surfaces. This theory is based on the key assumption that the in-plane momentum of SPPs, k_{spp}, is a conserved quantity for the propagation of SPPs over a patterned metal guiding structure. This point was validated by a direct comparison of our simulated results with double-slit diffraction images obtained with a PSTM. Most notably, and unlike previous reports[11], this work predicts the existence of an effective diffraction limit for lateral confinement on metal stripe waveguides. This has important implications for photonic systems and how they interface with electronic devices, which can be deeply subwavelength in dimension[5]. Nanoscale photonic systems will therefore have to rely on more strongly confining

SPP waveguides that exhibit a deeply subwavelength optical mode. It is worth mentioning that the notion of a diffraction limit for stripe waveguides is not in disagreement with the existence of such strongly guiding SPP waveguides that allow for short-distance information transport[2,3,24–26] (see Supplementary Information). However, our evidence for such a limit demonstrates that combined experimental and theoretical studies are absolutely essential to determine whether a metallic waveguide can support a subwavelength optical mode. Most generally, the SPP analogy to the double-slit experiment provides a new and intuitive vantage point from which to further examine the physics of SPPs and to explore new plasmonic device geometries.

Received 18 April 2007; accepted 18 June 2007; published 1 July 2007.

References

1. Barnes, W. L., Dereux, A. & Ebbesen, T. W. Surface plasmon subwavelength optics. *Nature* **424,** 824–830 (2003).
2. Bozhevolnyi, S. I., Volkov, V. S., Devaux, E., Laluet, J. Y. & Ebbesen, T. W. Channel plasmon subwavelength waveguide components including interferometers and ring resonators. *Nature* **440,** 508–511 (2006).
3. Takahara, J., Yamagishi, S., Taki, H., Morimoto, A. & Kobayashi, T. Guiding of a one-dimensional optical beam with nanometer diameter. *Opt. Lett.* **22,** 475–477 (1997).
4. Takahara, J. & Kobayashi, T. Low-dimensional optical waves and nano-optical circuits. *Opt. Photonics News* **15,** 54–59 (2004).
5. Zia, R., Schuller, J. A., Chandran, A. & Brongersma, M. L. Plasmonics: the next chip-scale technology. *Mater. Today* **9,** 20–27 (July/August 2006).
6. Pendry, J. B. Negative refraction makes a perfect lens. *Phys. Rev. Lett.* **85,** 3966–3969 (2000).
7. Ebbesen, T. W., Lezec, H. J., Ghaemi, H. F., Thio, T. & Wolff, P. A. Extraordinary optical transmission through sub-wavelength hole arrays. *Nature* **391,** 667–669 (1998).
8. Fang, N., Lee, H., Sun, C. & Zhang, X. Sub-diffraction-limited optical imaging with a silver superlens. *Science* **308,** 534–537 (2005).
9. Liedberg, B., Nylander, C. & Lundstrom, I. Surface plasmon resonance for gas detection and biosensing. *Sens. Actuators* **4,** 299–304 (1983).
10. Young, T. *A Course of Lectures on Natural Philosophy and the Mechanical Arts* (J. Johnson, London, 1807).
11. Krenn, J. R. *et al.* Non-diffraction-limited light transport by gold nanowires. *Europhys. Lett.* **60,** 663–669 (2002).
12. Weeber, J. C., Lacroute, Y. & Dereux, A. Optical near-field distributions of surface plasmon waveguide modes. *Phys. Rev. B* **68,** 115401 (2003).
13. Zia, R., Schuller, J. A. & Brongersma, M. L. Near-field characterization of guided polariton propagation and cutoff in surface plasmon waveguides. *Phys. Rev. B* **74,** 165415 (2006).
14. Joensson, C. Elektroneninterferenzen an mehreren kunstlich hergestellten feinspalten. *Z. Phys.* **161,** 454–474 (1961).
15. Keith, D. W., Ekstrom, C. R., Turchette, Q. A. & Pritchard, D. E. An interferometer for atoms. *Phys. Rev. Lett.* **66,** 2693–2696 (1991).
16. Schouten, H. F. *et al.* Plasmon-assisted two-slit transmission: Young's experiment revisited. *Phys. Rev. Lett.* **94,** 053901 (2005).
17. Zia, R., Selker, M. D. & Brongersma, M. L. Leaky and bound modes of surface plasmon waveguides. *Phys. Rev. B* **71,** 165431 (2005).
18. Burke, J. J., Stegeman, G. I. & Tamir, T. Surface-polariton-like waves guided by thin, lossy metal films. *Phys. Rev. B* **33,** 5186–5201 (1986).
19. Zia, R., Chandran, A. & Brongersma, M. L. Dielectric waveguide model for guided surface polaritons. *Opt. Lett.* **30,** 1473–1475 (2005).
20. Anemogiannis, E., Glytsis, E. N. & Gaylord, T. K. Determination of guided and leaky modes in lossless and lossy planar multilayer optical waveguides: reflection pole method and wavevector density method. *J. Lightwave Technol.* **17,** 929–941 (1999).
21. Boltasseva, A. *et al.* Integrated optical components utilizing long-range surface plasmon polaritons. *J. Lightwave Technol.* **23,** 413–422 (2005).
22. Karalis, A., Lidorikis, E., Ibanescu, M., Joannopoulos, J. D. & Soljacic, M. Surface-plasmon-assisted guiding of broadband slow and subwavelength light in air. *Phys. Rev. Lett.* **95,** 063901 (2005).
23. Goodman, J. *Introduction to Fourier Optics* (McGraw-Hill, New York, 1988).
24. Veronis, G. & Fan, S. H. Bends and splitters in metal–dielectric–metal subwavelength plasmonic waveguides. *Appl. Phys. Lett.* **87,** 131102 (2005).
25. Veronis, G. & Fan, S. H. Guided subwavelength plasmonic mode supported by a slot in a thin metal film. *Opt. Lett.* **30,** 3359–3361 (2005).
26. Pile, D. F. P. *et al.* Two-dimensionally localized modes of a nanoscale gap plasmon waveguide. *Appl. Phys. Lett.* **87,** 261114 (2005).

Acknowledgements

This work was supported by a DoD MURI sponsored by the AFOSR (F49550-04-10437) and an NSF Career Award (ECS-0348800). The authors thank Mark D. Selker, Jon A. Schuller and Anu Chandran for helpful discussions.
Correspondence and requests for materials should be addressed to M.L.B.
Supplementary information accompanies this paper on www.nature.com/naturenanotechnology.

Author contributions

R.Z. and M.L.B. conceived the experiments together. R.Z. conducted the experiments and simulations. R.Z. and M.L.B. co-wrote the manuscript.

Competing financial interests

The authors declare no competing financial interests.